International Journal of ITS Research, Vol. 1, No. 1, December 2003

A Study on Reliable Intelligent Vehicle Driving System by Using Features of Electric Vehicles
-Lane Keeping by Traction-Force-Distribution Control-

Naohisa Hashimoto Manabu Omae Hiroshi Shimizu
Keio University
(144-8 Ogura, Saiwai-ku, Kawasaki-shi,
Kanagawa, 212-0054, Japan
TEL: +81-44-580-1565,
E-mail: mocch@sfc.keio.ac.jp
omae@sfc.keio.ac.jp
hiros@sfc.keio.ac.jp)

Intelligent vehicle systems, such as the automatic driving system are expected to be the solution of current traffic problems. The key of those systems is reliability. This paper investigates a possibility of improving reliability by using the features of an electric vehicle (EV). EV with two motors can generate traction forces independently at left and right wheels and can control yaw moment adequately when a steering system is broken. The turning performance is evaluated in respect to vehicle's velocity, difference of traction forces, and steering condition by simulations and experiments. It is clarified that the lane-keeping can be realized by traction-force-distribution control. A lane-keeping controller by distribution of traction forces is proposed and validated by simulations. The fruit of this study improves reliability of automatic driving and shows the EV's advantage towards future vehicle systems.

Keywords: *Motion Control, Measurement and Control, Automobile, Intelligent Transport Systems, Electric Vehicle, Lateral Control, Vehicle Control, Vehicle Dynamics, Advanced Vehicle Control Safety Systems*

1. Introduction

This paper is concerned with lane-keeping control by distribution of traction forces of an electric vehicle (EV) with more than two motors[1][2]. There has been a great interest in the development of intelligent or automated highway systems[3][4][5][6]. Such intelligent transportation systems are expected to improve safety, efficiency, and accessibility of transit and quality of highway travel. The one of the crucial requirements of intelligent systems such as automatic driving systems or drive-by-wire systems is reliability of the system. One of the methods to improve the reliability is making the sensing and actuating system configured redundantly. It is relatively easy to realize redundant configuration of sensing system by multiplexing the various types of sensors. On the other hand, actuating system is difficult to configure redundantly.

An EV with more than two motors has a potential for coping with the above difficulty. One of the features of the EV with more than two motors is that traction force as well as braking force of each wheel can be controlled independently. In the case where a brake system is broken, the vehicle may decelerate by using the electric brake of the motor. In the case where one of the drive motors is broken, the vehicle may continue driving by the other motor and adequate steering for controlling yaw moment. In the case where a steering system of the vehicle is broken, the vehicle can avoid lane departure by generating adequate yaw moment by distribution of traction forces (see, Fig.1). This study focuses on the last case of the above. This study is aiming at realizing redundant configuration of lateral control system for an automatic driving system or a drive-by-wire system. Simulations and experiments are conducted for investigating the possibility of generating yaw moment enough to avoid lane departure by distribution of traction forces. Also a lane-keeping controller by distribution of traction forces is designed and validated by simulations.

There has been significant researches on lateral motion control by controlling EV's motors independently[7][8]. The control objective of those studies is improving stability of the vehicle in a critical condition. In the field of engine vehicles, Direct Yaw Moment Control (DYC) systems such as Vehicle Stability Control (VSC) have contributed to safety as practical systems. Those systems improve stability of the vehicle by reducing side-slip by controlling braking forces independently. The proposed control is different from the above studies and systems in the point that it is aiming at not reducing side-slip of the vehicle but keeping a lane at a constant velocity.

This paper is organized as follows: In chapter 2, simulations and experiments are conducted for investigating the relationship between the distributed traction forces and the turning radius of the vehicle. The results show that the vehicle has a possibility to realize lane-keeping on highway roads by adequate distribution of traction forces. In chapter 3, a lane-keeping controller by distribution of traction forces is designed. It is assumed that vehicle can obtain information of lateral deviation from road center and yaw rate by sensors. The control algorithm for calculating traction force of each wheel is proposed. Step response and tracking performances on a course with various radiuses of curvature are evaluated by simulations. In chapter 4, concluding remarks are described.

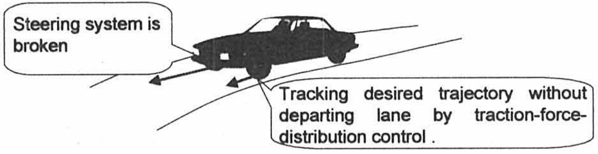

Figure 1. Lane-keeping by traction-force-distribution control

2. Investigation of turning performance by distribution of traction forces

This chapter investigates the relationship between distributed traction forces and turning radius by simulations and experiments.

2.1. Evaluation by simulations

The relationship between distributed traction forces and turning radius is evaluated.

If a turning radius of R[m] is realized by distribution of traction forces, this result provides a possibility of realizing lane-keeping control on the road whose radius of curvature is more than R[m]. In the following subsections, vehicle model, method of the simulations and simulation results are explained.

2.1.1. Vehicle model. Figure 2 shows a vehicle model with two motors. The vehicle model contains characteristics of self-aligning torque of front wheels, and characteristics of vertical load at an each tire according to lateral acceleration. The parameters of the model are based on a convert EV (see, Fig.3) constructed in our laboratory and used in the experiments. The longitudinal and lateral dynamics are modeled as follows:

$$m\dot{V} = T_r + T_l - RES(V) \cdots\cdots\cdots (1)$$

$$m\dot{V}(\gamma + \dot{\beta}) = C_{fl} + C_{fr} + C_{rl} + C_{rr} \cdots\cdots (2)$$

where,
m : vehicle mass,
V : longitudinal velocity,
γ : yaw rate,
β : side-slip angle at CG,
C_{fl}, C_{fr}, C_{rl} and C_{rr} : cornering forces at front-left, front-right, rear-left and rear-right tires,
T_l and T_r : traction forces at front-left and front-right tires,
RES : rolling resistance and aerodynamic drag.

Yaw dynamics are modeled as follows:

$$I\dot{\gamma} = l_f(C_{fl} + C_{fr}) - l_r(C_{rl} + C_{rr}) + \frac{1}{2}l_t(T_r - T_l) \cdot\cdot (3)$$

where,
I : yaw inertia of vehicle,
l_f: distance between CG and front axle,
l_r: distance between CG and rear axle,
l_t : distance between front-left tire and front-right tire (tread).

Cornering forces are determined by a saturation function with respect to side-slip angle and vertical load at each tire. The saturation function is modeled based on the literature[9].

Steering dynamics under unfixed condition is modeled as follows:

$$I_s\ddot{\delta} = SAT - C_s\dot{\delta} - FRC \cdots\cdots (4)$$

where,
I_s : inertia of steering linkage,
δ : steering angle,
C_s : damping coefficient of steering system,
SAT : self-aligning torque,
FRC : friction force.

Self-aligning torque (SAT) is determined by a side-slip angle at each front tire. The relationship between self-aligning torque and side-slip angle is modeled based on the literature[9].

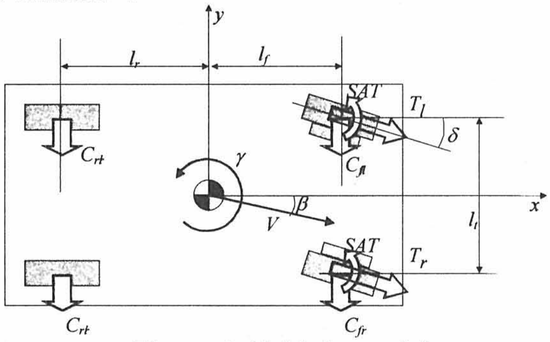

Figure 2. Vehicle model

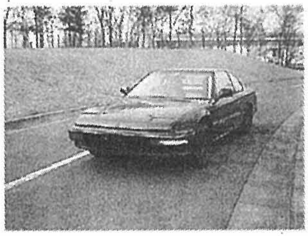

Figure 3. Convert EV

2.1.2. Method of simulations. Two kinds of simulation are conducted, which are called as simulation #1 and simulation #2 respectively. Simulation #1 is conducted to investigate the relationship between velocity and turning radius under constant traction force. Simulation #2 is conducted to investigate the relationship between the amount of traction forces and turning radius at a constant velocity.

In simulation #1, the front right wheel is controlled to generate traction forces of 600[N] or 1200[N], and the velocity is changed from 1[m/s] to 20[m/s]. The traction force of front left wheel is regulated to maintain a constant velocity. If the value of traction force is less than zero, the wheel generates braking force by an electric or a hydraulic brake.

In simulation #2, the front right wheel is controlled to generate traction forces from 0[N] to 1200[N]. The velocity is kept constant at 20[m/s], and the traction force of front left wheel is regulated to maintain a constant velocity.

In the above two simulations, the following two cases are assumed and evaluated. One case is that steering linkage is locked so that steering angle is fixed to be zero. This case called as steering is fixed. The other case is that steering linkage is not locked and front wheels are steered according to self-aligning torque generated by side-slips of the tires. This case called as steering is unfixed.

2.1.3. Results of simulations. Figures 4 and 5 show the results of simulation #1. The results show that the vehicle has different turning characteristic between cases of fixed steering angle and unfixed steering angle.

In the case where the steering angle is unfixed, the front wheels are steered by self-aligning torque. The direction of the steering is changed according to the velocity. At very low speeds, the front wheels turned to the direction where larger yaw moment is generated, resulting in a smaller turning radius. As the velocity is increased, the steering wheel angle is decreased, and at 14[m/s], the steering angle is at zero. At high speeds, the front wheels are so steered as to reduce yaw moment.

In the case where the steering angle is fixed, the change of turning radius is relatively small according to the velocity. Turning radius of 220[m] is realized at a speed of 20[m/s] with 1200[N] of a front-right wheel's traction force. This result shows that the vehicle has a possibility to realize lane-keeping on high way roads by adequate distribution of traction forces.

Figure 6 shows the result of simulation #2. This result shows the relationship between traction forces and turning radius. The reason for large turning radius at unfixed steering condition is that the front wheels are steered in the opposite direction of turning and the yaw moment is reduced at a speed of 20[m/s].

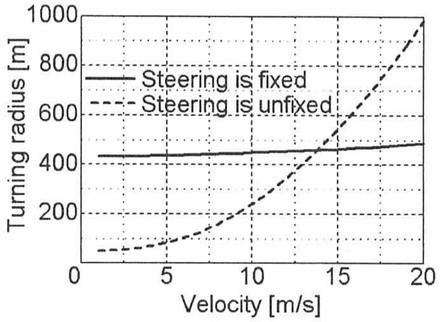

Figure 4. Relationship between velocity and turning radius (Maximum traction force is 600[N])

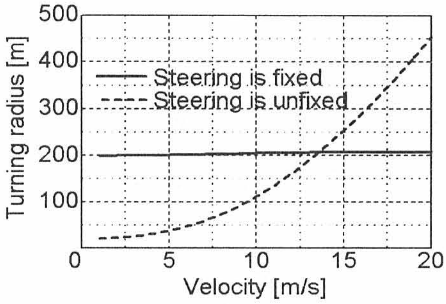

Figure 5. Relationship between velocity and turning radius (Maximum traction force is 1200[N])

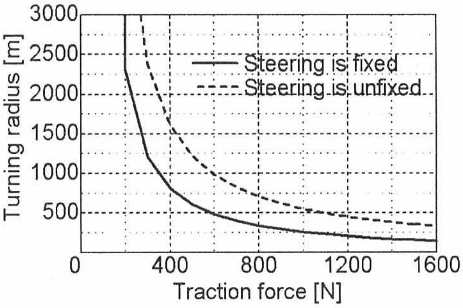

Figure 6. Relationship between maximum traction forces and turning radius

2.2. Evaluation by experiments

This section investigates the validity of simulation results. In the following subsections, method of experiments and experimental results are explained.

2.2.1. Method of experiments. In the experiments, a convert EV shown in Fig.3 is used. The experimental vehicle has two DC motors, each of which drives a front -left wheel and a front-right wheel. Two motors can be controlled independently. A yaw rate sensor, a velocity sensor, electric current sensors and electric voltage sensors are used for measurement.

In the experiments, only one of the two motors drives. Experiments are conducted under the following two conditions; in the first condition, the steering linkage is fixed so that the steering angle is fixed to be zero. In this condition, the steering wheel angle is fixed by the driver. In the second situation, the steering wheel angle is unfixed, and the front wheels are steered according to self-aligning torque. The velocity is kept constant by driver's braking. The experiments are conducted at a speed of 1[m/s]~13[m/s].

2.2.2. Result of experiments. Figures 7 and 8 show the results of the experiments. The simulation results under the same conditions as experiments are also plotted in the graphs. The results show the relationship between velocity and turning radius. The conditions of simulations are modified from those in section 2.1; the vehicle's velocity is kept by braking of four wheels and traction force by the motor is determined from the actual amount of the electric current and the voltage that supplied to the motor.

Seeing the results of unfixed steering condition, turning radius is small at low speeds, and it tends to become larger as a velocity increases. The reason of this result is that the front wheels are so steered by self-aligning torque as to reduce yaw moment as a velocity increases. The experimental result is different with the simulation result to some degrees, but experimental and simulation results correspond with each other qualitatively.

Seeing the results of fixed steering condition, the change of turning radius is relatively small. The experimental result is different with the simulation result to some degrees, but experimental and simulation results correspond with each other qualitatively. Thus the validity of simulations is clarified.

It should be noted the following; in the experiments, traction force on one-side wheel is relatively small, and braking force is act on four wheels in order to maintain a constant velocity. This influences the turning radius to become larger than the result in section 2.1. If the traction force is larger and braking force is controlled independently, it is expected that the turning radius comparable to the result in section 2.1 is realized in practical condition.

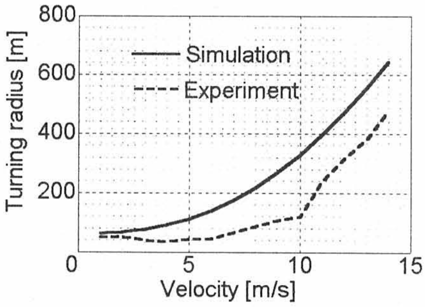

Figure 7. Comparison simulations with experiments at steering angle being unfixed

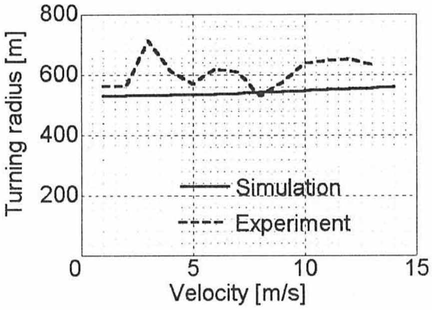

Figure 8. Comparison simulations with experiments at steering angle being fixed

3. Lane-keeping control by distribution of traction forces

There is a possibility that the vehicle keeping a lane of highway by distribution of traction forces, considering the result of chapter 2. This chapter explains an algorithm of lane-keeping control by distribution of traction forces. The algorithm is also evaluated by simulations.

3.1. Control algorithm

The objective of the algorithm is to determine the traction forces of right and left wheels to track the desired course. Traction forces of right and left wheels are calculated using the future and present lateral deviation from the center of the road. The future position of the vehicle is estimated using the current velocity and yaw rate of the vehicle. The lateral deviation is assumed to be obtained by the use of vision systems, magnetic sensors, and so on.

Figure 9 shows the variable used in the algorithm. Assuming that the controlled vehicle travels at a constant velocity and yaw rate, a estimated future lateral displacement (y_{vf}) in t_p[s] is given by:

$$y_{vf} = \frac{1}{2} V \cdot \gamma \cdot t_p{}^2 \quad \cdots\cdots\cdots (5)$$

To reduce future lateral deviation of the controlled vehicle from the desired course (y_{vf} - y_{cf}) to zero, the required change of yaw rate ($\Delta\gamma_{des}$) should satisfy the following equation:

$$y_{cf} = \frac{1}{2} V (\gamma + \Delta\gamma_{des}) \cdot t_p{}^2 \quad \cdots\cdots\cdots (6)$$

From the equation above, the required change of yaw rate is given by:

$$\Delta\gamma_{cf} = \frac{2 \cdot y_{cf}}{V \cdot t_p{}^2} - \gamma \quad \cdots\cdots\cdots (7)$$

The amount of difference of traction force (T_d) is determined using $\Delta\gamma_{des}$ and a present lateral deviation (ε) as follows:

$$T_d = K_1 \cdot \Delta\gamma_{des} + K_2 \cdot \varepsilon \quad \cdots\cdots (8)$$

In the above equation, the former part is the feed-forward term and the latter is the feedback term. K_1 and K_2 are constant gains. K_1 and K_2 are determined to be the values that minimize J by simulations.

$$J = \int_0^{T_{sim}} \varepsilon^2 dt \cdot\cdot\cdot\cdot\cdot\cdot\cdot\cdot\cdot (9)$$

In a practical system, K_1 and K_2 will be tuned by road tests. To keep a constant velocity, total traction force (T_n) is equal to rolling resistance and aerodynamic drag ($RES(V)$). So, traction forces of right and left wheels are given by:

$$T_n = RES(V) \cdot\cdot\cdot\cdot\cdot\cdot\cdot\cdot (10)$$

$$T_r = \frac{T_n + T_d}{2},\ T_l = \frac{T_n - T_d}{2} \cdot\cdot\cdot\cdot\cdot\cdot (11)$$

When the value of traction force is less than zero, the wheel generates braking force by an electric or hydraulic brake. If the derived traction force of one wheel is more than maximum traction force of the wheel, the traction force of the other wheel is given by:

$$T_r = T_{max} - T_d, T_l = T_{max} \cdot\cdot\cdot\cdot\cdot\cdot\cdot (12)$$

or

$$T_l = T_{max} - T_d, T_r = T_{max} \cdot\cdot\cdot\cdot\cdot\cdot\cdot (13)$$

In this case, it is impossible to keep a constant velocity, resulting in decrease of a velocity.

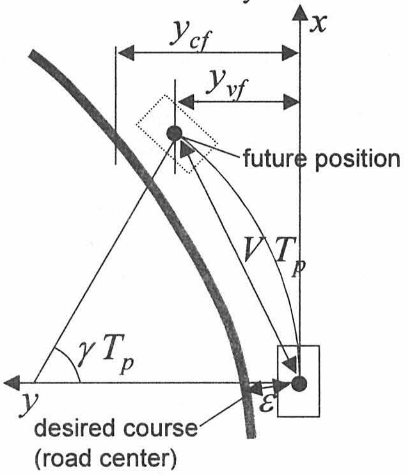

Figure 9. Control algorithm

3.2. Evaluation of lane-keeping control by distribution of traction forces

In this section, the proposed control algorithm is evaluated by simulations using. The following subsections describe simulation results of step response, lane-keeping performance on courses with constant curvature and lane-keeping performance on a course with various curvatures.

3.2.1. Evaluation of step response. Step response is investigated. The simulation is conducted under the following conditions. The vehicle travels on the straight road with a lateral deviation of 1[m] at a speed of 20[m/s]. The maximum and minimum traction force is 1200[N] and -1200[N] respectively.

Figures 10 and 11 show simulation results of traction forces of right and left wheels, and lateral deviation respectively. The result shows that lateral deviation converges to zero for 5[s].

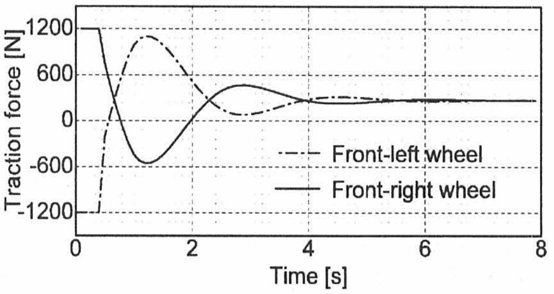

Figure 10. Traction forces at step response

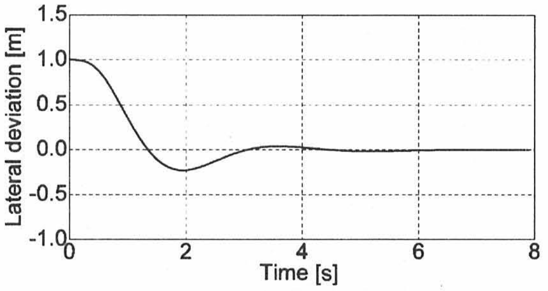

Figure 11. Lateral deviation at step response

3.2.2. Evaluation of lane-keeping performance on courses with constant curvature. The lane-keeping performance on courses with a constant curvature is investigated. The radiuses of curvature are 150[m], 200[m], 300[m], 400[m] and 500[m]. The maximum and minimum traction force is 1200[N] and -1200[N] respectively. The vehicle's speed is 20[m/s]. Each course has a straight section (150[m]) and a curved section. The vehicle travels on the straight section firstly, and then travels the curved section.

Figure 12 shows the maximum lateral deviations at each curvature. Figures 13, 14, 15 and 16 show traction forces and lateral deviation at the courses of curvature of 200[m] and 400[m]. Since the vehicle cannot generate enough yaw moment due to the limitation of the traction force, the lateral deviation is very large at 150[m]. The simulation result of section 2.1 shows that 1200[N] of traction force is necessary to achieve a turning radius of 220[m] at a speed of 20[m/s]. The lateral deviation at radius of curvature of 200[m] is relatively small, although 1200[N] of traction force is necessary to achieve a turning radius of 220[m] at a speed of 20[m/s]. The reason for the small lateral deviation is due to the decrease of the vehicle speed caused by the limitation of the traction force. At low speeds, smaller turning radius is achieved, resulting in better lane-keeping performance. The lateral deviations at curvatures larger than 200[m], are less than 0.6[m], which is small enough to avoid lane departure.

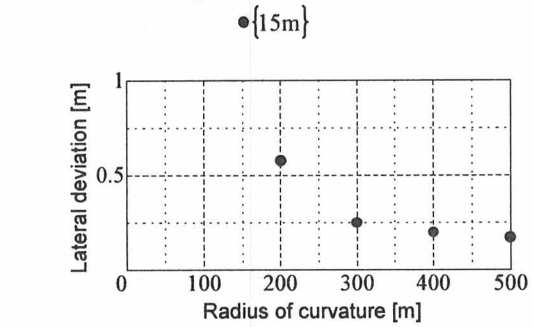

Figure 12. Simulation result (maximum lateral deviation with respect to radius of curvature)

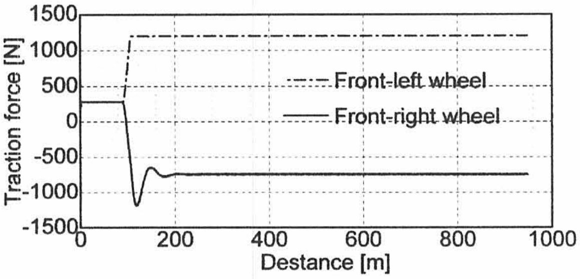

Figure 13. Simulation result (Traction forces at R=200[m])

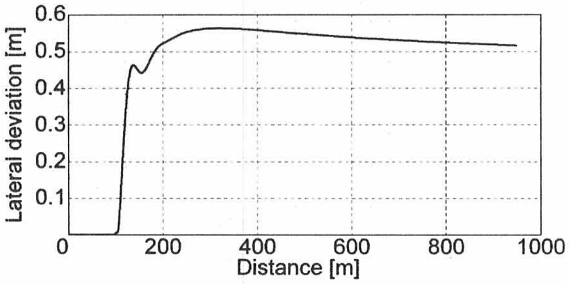

Figure 14. Simulation result (Lateral deviation at R=200[m])

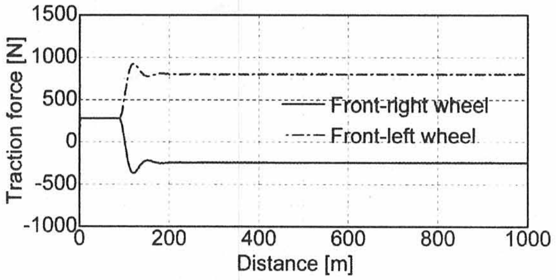

Figure 15. Simulation result (Traction forces at R=400[m])

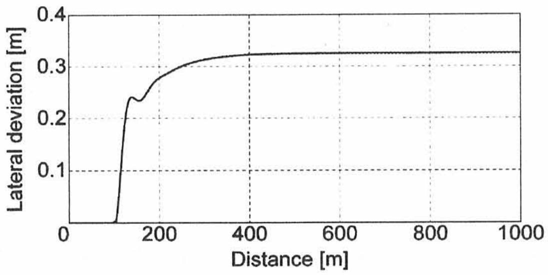

Figure 16. Simulation result (Lateral deviation at R=400[m])

3.2.3. Evaluation of lane-keeping performance on course with various curvatures. Lane-keeping performance on a course with various curvatures is investigated. The course is composed of a combination of curves with radius of 640[m], 320[m], 160[m] and 105[m], as shown in Fig.17. The maximum and minimum traction force is 1200[N] and -1200[N] respectively. The vehicle's speed is 20[m/s].

Figures 18, 19 and 20 show the results of simulations. Figure 18 shows the lateral deviation. As the turning radius becomes smaller, the lateral deviation becomes larger. However, lateral deviation is less than 0.8[m] if the vehicle is able to turn using only the traction force. Figure 19 shows the traction forces. Traction forces are generated to track the course. Traction force is max at the third and forth curves. Figure 20 shows the velocity. Vehicle's velocity is kept constant until the vehicle enters the third curve, but at the third corner, the velocity is decreased due to limitation of traction force. These results show that the proposed lane-keeping controller is valid under the transient condition if the radius of curvature of a corner is more than the turning radius achieved by distribution of traction forces.

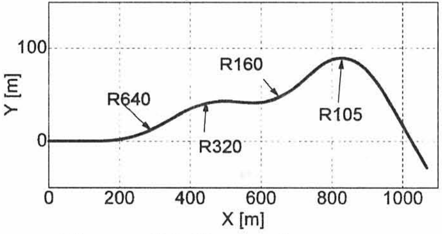

Figure 17. Desired course

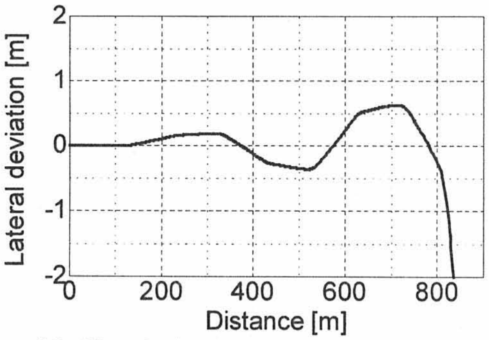

Figure 18. Simulation result (Lateral deviation)

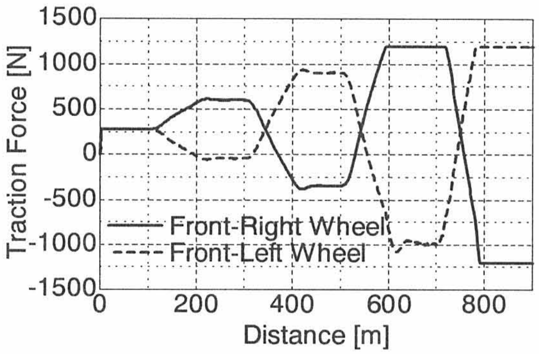

Figure 19. Simulation result (Traction forces)

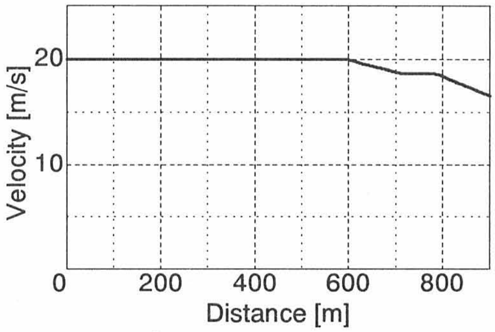

Figure 20. Simulation result (Velocity)

4. Conclusions

Lane keeping by distribution of traction forces of EV with more than two motors is investigated. Simulations and experiments are conducted for investigating a possibility of generating yaw moment enough to keep a lane by distribution of traction forces. The relationship among turning radius, distributed traction forces and velocity is clarified quantitatively, which shows the possibility of lane-keeping on highway road by distribution of traction forces. A lane-keeping controller is proposed and validate by simulations. The proposed control system realizes redundant configuration of lateral control system for automatic driving system and steer-by-wire system by combining with a steering control system. The fruit of this study improves reliability of automatic driving system, drive-by-wire system and so on, and shows the EV's advantage towards future vehicle systems.

This study is conducted with using one type of vehicle and vehicle model and under the conditions of dry road. It is important to investigate the relationships between turning performance and vehicle characteristics, tire characteristics and road conditions. One of the future works is to clarify the above relationships by simulation and experiments. We also plans to carry out lane-keeping control by experiments using EV with more than two motor and sensors to obtain the relative position of the vehicle from the course such as vision sensors and RTK-GPS.

References

[1] H. Shimizu, S. Matsugaura, K. Kawakami and Y. Kondo, "A new concept electric vehicle 'Luciole'", Proceedings of 1998 FISITA World Automot, 1998, CD-ROM.

[2] S. Matsugaura, K. Kawakami and H. Shimizu, "Development of New Concept Electric Vehicle 'KAZ'", Proceedings of AVEC'02, 2002, pp.821-825.

[3] S. Tsugawa, H. Mori, S. Kato, "A Lateral Control Algorithm for Vision-Based Vehicles with a Moving Target in the Field of View", Proceedings of IEEE Intelligent Vehicles Symposium, 1998, pp.41-45.

[4] M. Omae, H. Shimizu and N. Hashimoto, "Traction-Force-Distribution Control of EV with In-Wheel-Motors for Lane Keeping", Proceeding of EVS-18, 2001, CD-ROM.

[5] M. Omae, H. Shimizu and T. Fujioka, "Vehicle Motion Control for Fully Automatic Driving in Local Area", Proceedings of AVEC'02, 2002, pp.457-462.

[6] J. Tanaka, et. al., "Workload of Using Driver Assistance System, Proceedings of 2000 JSAE Annual Congress, 2000, pp.5-8, (in Japanese).

[7] S. Sakai and Y. Hori, "Lateral Motion Stabilization with Feedback Controlled Wheels-Experimental Studies with 4-Wheel Motored EV-", Proceedings of AVEC02, 2002, pp.815-820.

[8] D. Johnston, "TM4 motor-wheel drive and control system: Performance, benefits and advantages", EVS-17, 2000, CD-ROM.

[9] M. Abe, *VEHICLE DYNAMICS AND CONTROL*, Sankaidou, 1992, (in Japanese).

Naohisa Hashimoto is a Ph. D candidate of the Graduate School of Media and governance. He received master degree from the Keio University. His major interests are intelligent vehicle systems and image processing.

Manabu Omae is an assistant professor of the Facility of Environmental Information of Keio University. He received Ph. D from the University of Tokyo in 2000. His major research interests are AVCSS(Advanced Vehicle Control and Safety Systems) and electric vehicles.

Hiroshi Shimizu is a professor of the Facility of Environmental Information of Keio University. He received Ph. D from the Tohoku University in 1976. His major research interest is development of high performance electric vehicles.

Received: 21 March 2003
Revised: 18 August 2003
Accepted: 16 September 2003
Editor: Yoshihiro Suda